

Unveiling the dynamics of deep-focus earthquakes: Insights from the 2020 Jepara event Mw 6.7 and subduction processes beneath Java

Rudarsko-geološko-naftni zbornik (The Mining-Geology-Petroleum Engineering Bulletin) DOI: 10.17794/rgn.2025.5.5

Original scientific paper



Tio Azhar Prakoso Setiadi¹* № Anne Meylani Magdalena Sirait² № Aleksiel Halauwet³ № Andrean Vesalius Hasiholan Simanjuntak³,4 № Adi Susilo⁵,6 № Aleksiel Halauwet³ № Aleksiel Ha

- ¹ National Research and Innovation Agency, Bogor, 16911, Indonesia.
- ² Geophysics Program, Faculty of Mathematics and Natural Sciences, Universitas Indonesia, Depok, 16424, Indonesia.
- ³ Meteorological, Climatological, and Geophysical Agency (BMKG), Central Jakarta, Kemayoran, 10610, Indonesia.
- ⁴ Tsunami Disaster and Mitigation Research Center (TDMRC), University of Syiah Kuala, Banda Aceh, 231111, Indonesia.
- ⁵ Department of Physic, Faculty of Mathematics and Natural Sciences, Brawijaya University, Malang, 65145, Indonesia.
- ⁶ Research Study of Geosciences and Hazard Mitigation, Universitas Brawijaya, Malang, 65145, Indonesia.

Abstract

The 2020 Jepara earthquake (Mw 6.7) represents a significant deep-focus seismic event within the subducting Indo-Australian Plate beneath Java Island. This study investigates its characteristics using automatic moment tensor inversion and double-difference relocation based on seismic data from the Meteorology, Climatology, and Geophysics Agency (BMKG). A total of 1,899 earthquakes recorded between 2010 and 2022 were analyzed, focusing on events with a depth of up to 600 km. Moment tensor analysis revealed a normal faulting mechanism with two nodal planes: the first with a strike of 310°, dip of 59°, and rake of -68°, and the second with a strike of 92°, dip of 37°, and rake of -121°. The centroid depth was refined to 544 km, and the variance reduction (VR) exceeded 60%, which classifies the results as high-quality (Category A). Approximately 85% of the hypocenters were successfully relocated, improving root mean square (RMS) travel times to less than 1 second. The earthquake is associated with slab dehydration and the polymorphic phase transition of olivine to spinel under high pressure and temperature. These processes contribute to changes in fault mechanisms and the structural variation of the mantle transition zone. The findings enhance understanding of the deep-focus earthquakes beneath Java and can significantly contribute to future earthquake mitigation in Indonesia.

Keywords:

Java Island, deep-focus earthquakes, moment tensor inversion, double-difference relocation, slab dehydration

1. Introduction

Java Island experiences significant seismic activity due to active tectonic processes (Gunawan and Widiyantoro, 2021; Widiyantoro et al., 2020). These processes are primarily driven by the subduction of the Indo-Australian oceanic plate beneath the Eurasian continental plate at a rate of 5–6 cm/year. Additionally, active onshore faults with slip rates of 1–2 cm/year contribute to frequent and sometimes destructive earthquakes (Argus and Gordon, 1991; DeMets et al., 2010; Pasari et al., 2021a). Historically significant events include the 1994 Banyuwangi earthquake (Mw 7.8) (Abercrombie et al., 2001; Polet and Kanamori, 2000), the 2006 Pangandaran earthquake (Mw 7.8) (Kato et al., 2007; Ammon et al., 2006; Fujii and Satake, 2006), the 2006 Yogyakarta earthquake (Mw 6.0) (Saputra et al., 2021;

Received: 23 December 2024. Accepted: 24 April 2025.

Available online: 21 October 2025

Walter et al., 2008), and the recent 2020 Jepara earth-quake (Mw 6.0). The Jepara earthquake, occurring at a depth of 560 km, ranks as one of the largest deep earthquakes in the past decade, with its effects felt across Java (MMI IV–V) and extending to Sumatra, South Bali, and Lombok (MMI II–IV).

Deep earthquakes represent a complex geophysical phenomenon requiring detailed investigation. According to BMKG records, only 3% of earthquakes in the last decade were categorized as deep-focus events (see Figure 1). Tectonically, these earthquakes occur within subducting slabs, resembling shallow earthquakes superficially but differing significantly in their mechanisms (Li et al., 2018; Zhan, 2020). The deep hypocenters amplify seismic wave propagation, leading to pronounced shaking at distant locations, as observed in the 1998 Mexico earthquake (Mw 7.8) (Ramírez-Herrera and Orozco, 2002; Tibi et al., 2003). Deep earthquakes originate in dense, old oceanic slabs, which slow wave attenuation while enhancing wave propagation (Tibi et al., 2003; Wu and Takeo, 2004). These events can cause signifi-

^{*} Corresponding author: Tio Azhar Prakoso Setiadi e-mail address: tio.prakoso08@gmail.com

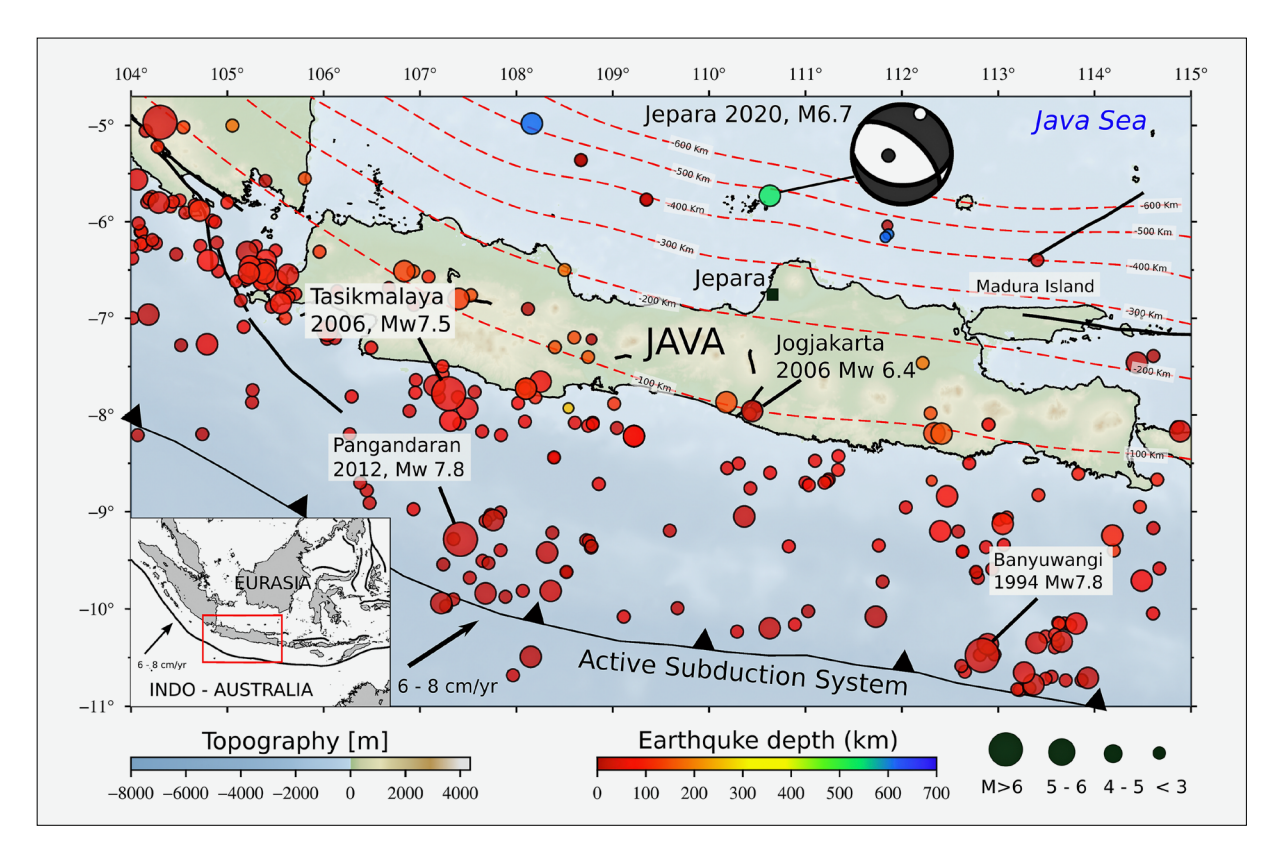


Figure 1. The seismicity and tectonic map of Java Island shows the distribution of felt earthquakes over the last 50 years. Notable strong and destructive earthquakes that occurred in the Java region include the Bantul 2006 M 5.9, Pangandaran 2006 M 7.7, Tasikmalaya 2009 M 7.0 and 2017 M 6.9, Lebak 2018 M 6.1, Banten 2019 M 6.9, Jepara 2020 M 6.7, and Malang 2021 M 6.1 earthquakes. The tectonics of Java Island are controlled by the subduction activity of the Indo-Australian Plate, subducting the Eurasian Plate at 6-8 cm/yr. Several active faults on Java Island, such as the Cimandiri, Lembang, Baribis, Kendeng, and Opak faults, also influence the island's seismicity. (Source: Fault data obtained from Pusgen 2017, Bathymetry from BATNAS BIG, and seismicity from the International Seismic Centre).

cant damage in distant regions, particularly in alluvial sediment areas, as exemplified by the 2007 Indramayu earthquake, which caused damage in Sukabumi.

Several studies have been published using full waveform to highlight an unknown active fault in Indonesia such as Tobelo Fault (Simanjuntak et al., 2023), Balantak Fault (Simanjuntak et al., 2024), onshore Sumatra backthrust (Muksin et al., 2023) and Cianjur Fault (Supendi et al., 2023). However, there is lack of studies concerning subduction activities, especially for intermediate and deep-focus earthquakes. Adi et al. (2024) studied the possible backthrust system in south-central Java at an intermediate depth while the 2020 Jepara earthquake occured in deep-focus in the northern part of Java. Several destructive earthquakes have produced a significant nowcasting earthquake score for most major cities in Indonesia especially in Java Island (Pasari et al., 2021b; Pasari et al., 2021c). Therefore, the 2020 Jepara earthquake raise an important question about the mechanism of deep-focus earthquake and its geodynamic process.

The 2020 Jepara earthquake was accompanied by subsequent events in Rangkasbitung, Enggano, and Pangandaran on the same day. The deep nature of the Jepara

earthquake likely triggered these follow-up earthquakes, which were widely felt by residents. This study aims to investigate the characteristics of the 2020 Jepara earthquake through analysis of earthquake catalogs and seismic records. Source mechanism analysis was conducted using automatic moment tensor inversion based on seismic data from stations across Java Island. Additionally, hypocenter relocation, employing travel-time data, was utilized to refine the earthquake locations and delineate the tectonic structure beneath Java. The findings from this study will contribute to understanding deep-focus earthquakes in Java, providing insight for both scientific research and disaster mitigation efforts.

2. Methods

The earthquake data utilized in this study was obtained from analyses conducted by the Meteorology, Climatology, and Geophysics Agency (BMKG). The dataset includes the travel times of seismic phases (P and S) recorded by all seismic stations within a range of 0°–5° latitude and longitude. A total of 1,899 earthquakes spanning a 13-year period (2010–2022) were analyzed. Data selection was based on specific criteria: an azi-

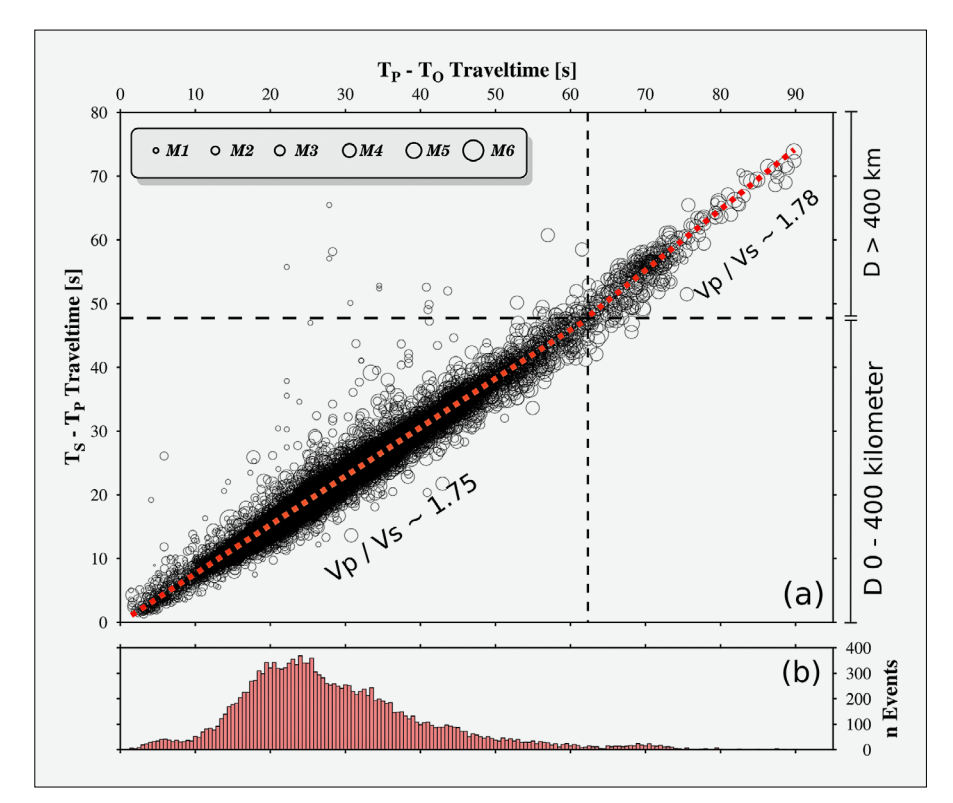


Figure 2. Wadati diagram showing the travel time distribution with two Vp/Vs ratios of 1.75 and 1.78. The highest number of phases is in the travel time range of Tp – To about 20 – 30 seconds with a total of 300 – 400 phases.

muthal gap of less than 200°, a minimum of 5 P-phase observations, 3 S-phase observations, and a depth range of 0–600 km. The travel time distribution revealed a Vp/Vs ratio of 1.75 for distances of 0–400 km and 1.78 for distances exceeding 400 km, as illustrated in **Figure 2**.

The earthquake mechanism was investigated using seismic wave recordings from BMKG stations. Hypocenter information for the Jepara earthquake, which occurred on July 7, 2020, at 05:54:44 WIB, was obtained from the BMKG catalog. The earthquake had an epicenter located at 6.12° S, 110.55° E, with a depth of 578 km and a magnitude of Mw 6.7. Seismic recordings were collected within a time window spanning 10 minutes before and 60 minutes after the event's origin time. These waveform data underwent several preprocessing corrections, including baseline correction to eliminate offsets, removal of instrument response to obtain true ground motion, and the application of a bandpass filter (0.02-0.08 Hz) to suppress low-frequency drift and high-frequency noise. After these corrections, the velocity signals were integrated into displacement for further analysis. To optimize processing time and maintain data quality, waveform data containing significant gaps or low signalto-noise ratios were excluded from the analysis.

2.1. Moment Tensor Inversion

In this study, we performed an automatic moment tensor inversion on the observed seismic waveforms. These waveforms represent a combination of the earthquake source mechanism and the propagation characteristics of the medium. The moment tensor solution was derived

using a weighted least-squares inversion approach, which minimizes the discrepancy between observed and synthetic waveforms (**Tarantola**, 2005).

The inversion process employed full-waveform data to analyze the characteristics of both body and surface waves. Signals with low signal-to-noise ratios (SNR) were excluded using a tapering technique. This technique was applied to a time window twice the duration of the difference in arrival times between the P and S waves (Sokos and Zahradnik, 2008; Vackář et al., 2017). An example of this signal tapering process at one of the seismic stations can be seen in Figure 3. Moment tensor inversion was performed over a spatial and temporal grid to determine the centroid location and time parameters of the earthquake. The grid model extended within a radius of 10-15 km from the initial hypocenter location, with depth intervals of 5-10 km and a time deviation of ± 5 seconds from the origin time. Synthetic signals were generated using a one-dimensional seismic velocity model that integrated the CRUST1.0 model for the crustal layer (Laske et al., 2013) and the AK135 model for the mantle layer (Kennett et al., 1995).

The quality of the moment tensor solutions was assessed using variance reduction (VR), a metric that quantifies the agreement between observed and synthetic waveforms. Based on VR values, the solutions were categorized into four quality classes: A, B, C, and D. Solutions with VR values of 20% or higher were considered acceptable, while those below 20% (Quality D) were deemed poor and excluded from further analysis. Quality A represented the most reliable centroid moment tensor (CMT) solutions, involving at least four stations

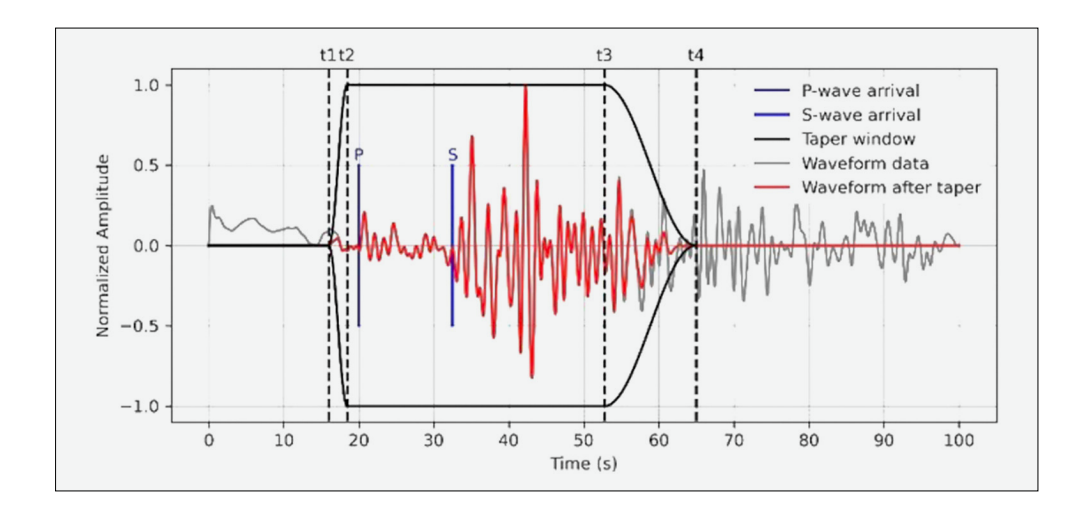


Figure 3. Illustration of signal tapering at one of the stations. The P phase (blue line) arrives at 20 seconds and the difference in S-P time is 12.5 seconds, both within the tapering window used in the moment tensor inversion process.

with a VR of approximately 60%. Quality B included solutions with three stations achieving a VR of 60% or four stations with a VR ranging from 40% to 60%. Quality C encompassed solutions with VR values between 20% and 40%, which were acceptable but less robust compared to Quality A and B.

2.2 Double Difference Relocation

The HypoDD program (Waldhauser, 2001) was employed in this study to perform double-difference relocation (Waldhauser and Ellsworth, 2000) for determining earthquake hypocenters. This method assumes that when the distance between two earthquake hypocenters is smaller than their distance to the recording station, their ray paths traverse a similar medium. HypoDD minimizes residuals between observed and calculated travel-time differences through an iterative process, refining earthquake locations and updating partial derivatives with each iteration as shown in the schematic cartoon in Figure 4.

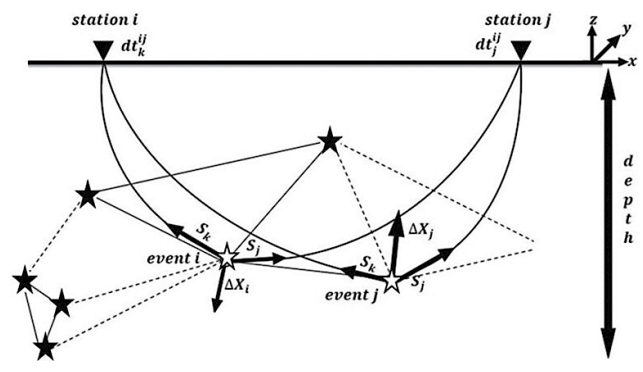


Figure 4. The schematic cartoon of relative relocation using HypoDD shows residuals between observed and calculated travel-time differences through an iterative process, refining earthquake locations and updating partial derivatives with each iteration (modified from Waldhauser and Ellsworth, 2000).

This method has been effectively utilized to relocate earthquakes in Indonesia using BMKG data, contributing to more precise earthquake locations and improved tectonic interpretations. Notable applications include studies in Indonesia (Nugraha et al. 2018; Setiadi et al. 2022). The relocation results from these studies have significantly advanced the understanding of tectonic structures in the region.

3. Results and Discussions

The automatic moment tensor inversion was successfully conducted using nine seismic sensors out of a total of fifteen. The inversion utilized data from three seismic wave components: vertical (Z), north-south (N), and eastwest (E). Seven sensors were excluded from the analysis due to low variance reduction (VR) quality and insufficient signal-to-noise ratio (SNR), which would have resulted in unsatisfactory solutions. Stations SNJI, TPI, and NKBI produced the most reliable solutions, with high VR values and minimal discrepancies between observed and synthetic waveforms. We applied the bandpass filter with range 0.02 - 0.08 Hz that is suitable with most seismic stations used. Example result from SNJI stations shows a good fitting between observation and synthetic waveform as shown in Figure 5. The SNJI seismic stations SNJI performs best fitting results than other stations. It can be stated that the synthetic model from Green's function model used are suitable with the geological condition as well as the bandpass frequency range.

Other stations, such as PRJI, BKJI, and BBJI, exhibited overlapping solutions between observations and synthetics, which were attributed to minor mismatches in the Green's function model. Despite this, these three stations provided reasonably good solutions, with VR values exceeding 20%. The moment tensor results yielded two nodal planes with the following parameters: the first nodal plane has a strike of 310°, a dip of 59°, and a rake of -68°, while the second nodal plane has a strike of 92°, a dip of 37°, and a rake of -121°.

The centroid depth was refined to 544 km from the initial estimate of 536 km. The earthquake magnitude derived from the moment tensor inversion was recalculated as Mw 6.7, slightly lower than the previously re-

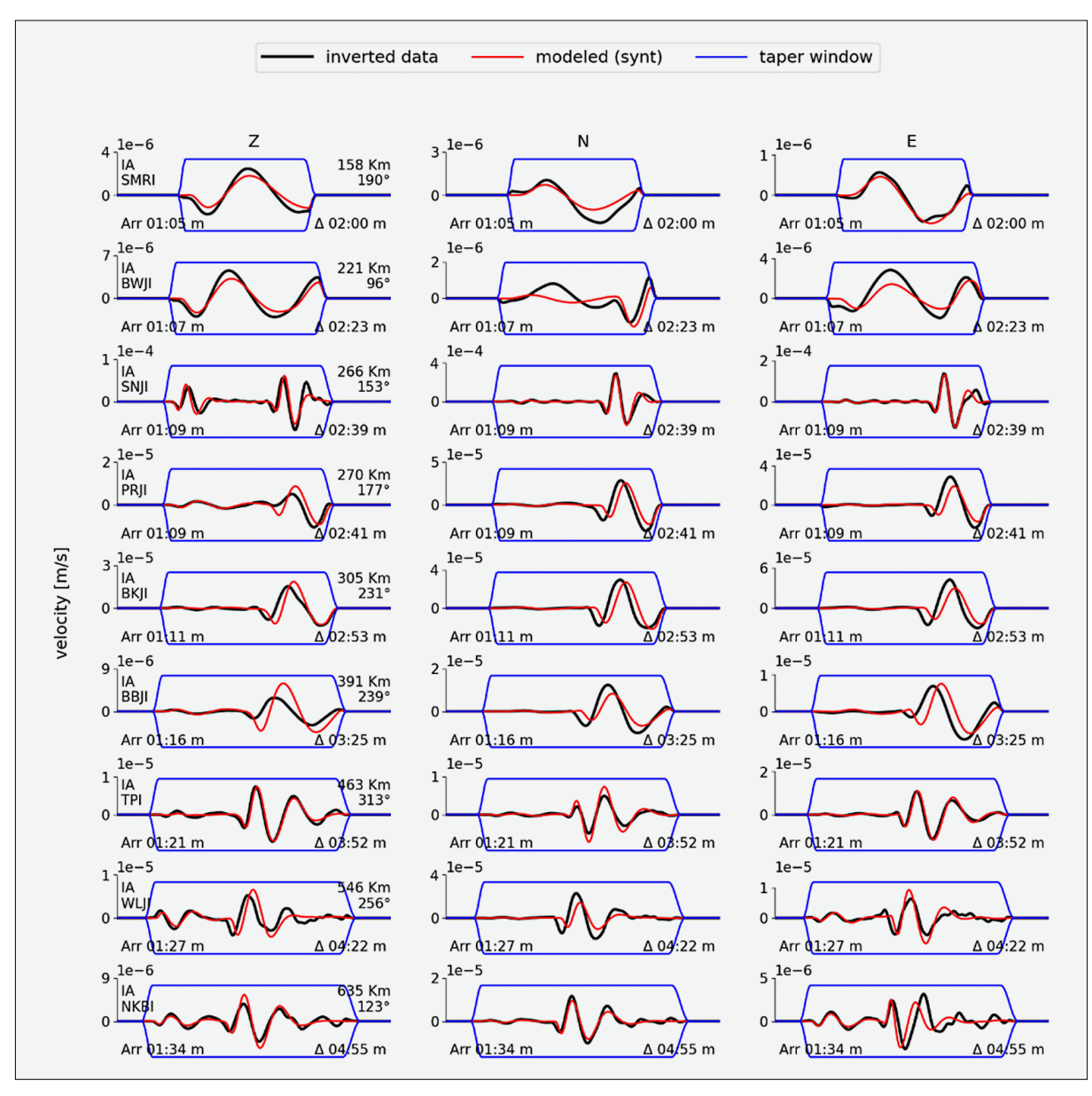


Figure 5. Results of the moment tensor inversion at 9 seismic stations used in this study. The inversion was carried out on the displacement signals on three components (Z, N, E). The black line represents the observed signal while the red line represents the synthetic signal generated through the Green's function model.

ported Mw 6.8. This magnitude was determined using longer wave periods, yielding stable and reliable results. The centroid time was adjusted by 4 seconds, changing from 07:54:46 to 07:54:50, due to the inclusion of all seismic waves from the available sensors. Statistically, the variance reduction (VR) quality of the moment tensor inversion results falls within category A, indicating a reliable centroid moment tensor (CMT) solution. This classification was based on a minimum of four stations achieving a VR value of approximately 60%. The results are consistent with those from other agencies, as shown in **Table 1**. However, the results from this study are considered more accurate due to the utilization of local seismic stations, which provided higher resolution data as shown in **Figure 6**.

The relocation results reveal significant changes in the root mean square (RMS) travel times of hypocenters, as illustrated in **Figure 7**. These adjustments indicate that the new hypocenter locations are more accurate and form distinct clusters that align well with the derived source mechanism solutions. Approximately 85% of the earthquakes were successfully relocated with consistent centroidal nodal depth (CND) solution values ranging from 40 to 80 during each iteration (**Waldhauser and Ellsworth, 2000**).

The relocated hypocenters were integrated with the source mechanism solutions, as shown in **Figure 8a**. To further analyze the distribution, a vertical cross-section was created to illustrate the spatial relationship between the relocated hypocenters and the source mechanisms,

providing insight into the characteristics of the 2020 Jepara earthquake. The vertical section along line A–A' (see **Figure 8b**) highlights the complex tectonic struc-

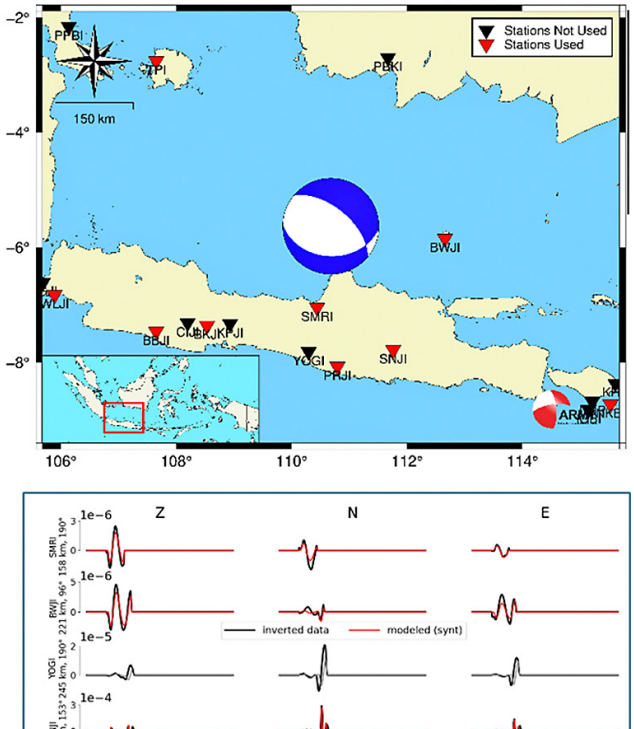


Figure 6. Map of seismic stations used (red triangles) and not used (black triangles), as well as the results of the source mechanism with normal faulting in the east-west strike direction (top panel). An example of waveform inversion results used, with stations showing the comparison of synthetic signals (red lines) used in the inversion, while others are not used due to having low VR (Variance Reduction) (bottom panel).

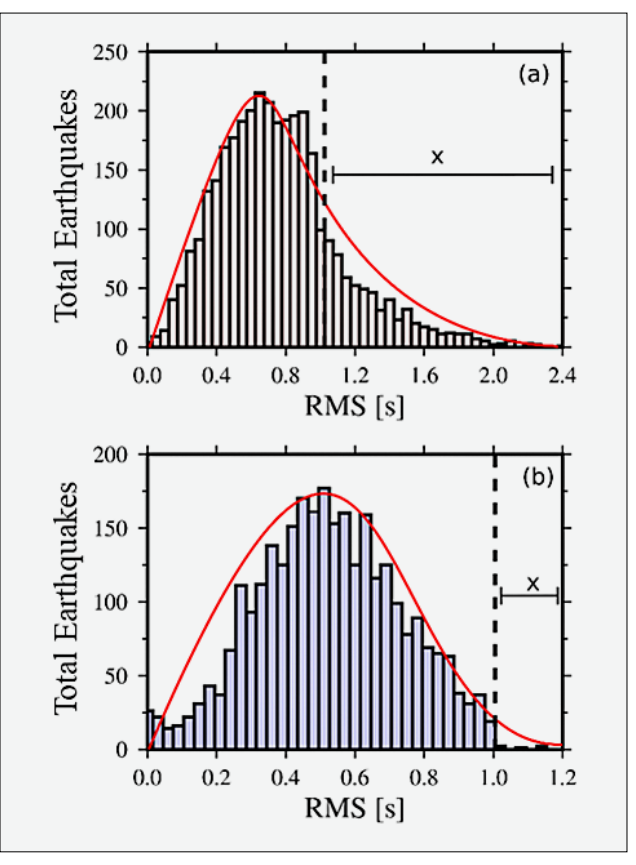


Figure 7. HypoDD relocation results shows the graph before relocation with RMS o - 2.4 s (a) and after relocation with most hypocenters with an improved RMS < 1.0 s(b).

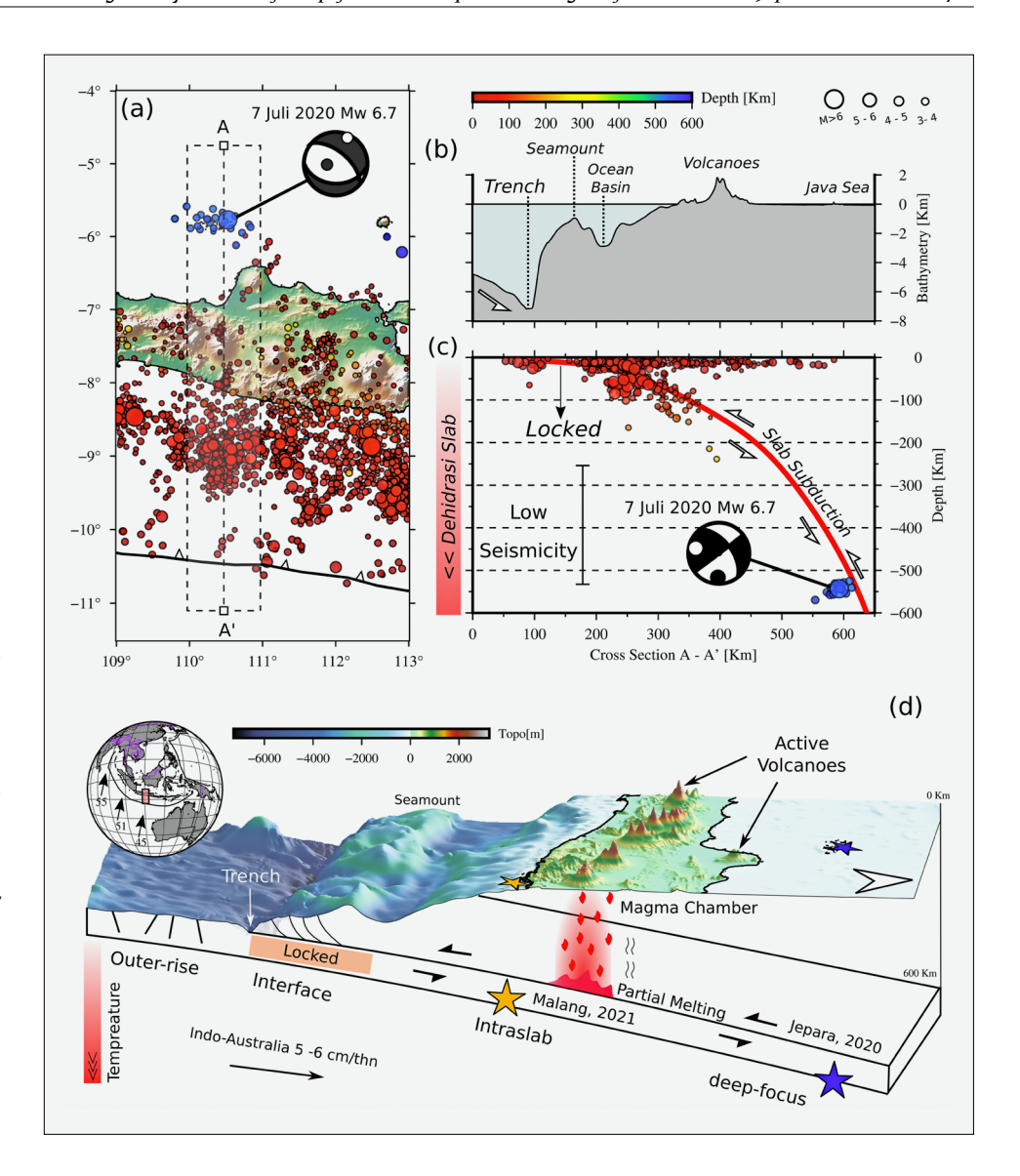
ture of Java Island, including features such as trenches, seamounts, and ocean basins formed by subduction processes. Additionally, the relocation results delineate earthquake clusters within the outer-rise, interface, intraslab, and deep-focus zones (see **Figure 8c**).

Vertical slice profiles reveal key seismic phenomena in Java Island, including locking at the interface zone and low seismicity at depths of 200–500 km. These features are associated with high coupling in the asperities of the Java subduction zone (Widiyantoro et al., 2020;

Table 1. Comparison of source mechanism results of the 2022 Malang earthquake between this study and other institutions (seismic moment (Mo) in the table is in units of 10¹⁹ Nm).

Result from	Nodal Plane	Longitude	Latitude	Magnitude (Mw)	Depth (km)	Seismic Moment (Mo)
USGS	301, 56, -72	110.68	-5.6	6.6	533	1.2
	91, 38, -114					
GFZ	316, 61, -61	110.64	-5.65	6.6	536	1
	86, 39, -131					
IPGP	310, 59, -69	110.67	-5.36	6.8	536	1.7
	97, 37, -121					
GCMT	313, 60, -67	110.69	-5.6	6.7	533	1.3
	92, 37, -124					
This study	310, 59, -68	121.45	-6.1	6.7	536	1.6
	97, 37, -121					

Figure 8. (a) Map showing the relocation results and source mechanisms of the 2020 Jepara earthquake. (b) Geological structures and formations resulting from the subduction process, with the vertical profile section A-A' illustrating the hypocenter distribution at depths of o-600 km. (c) Low seismicity observed at depths of 200-500 km is associated with increased temperature and pressure leading to slab dehydration. (d) The schematic diagram explains the subduction tectonics of Java Island, highlighting seismic activity in the outer-rise, interface, intraslab, and deep-focus zones. Geological formations such as trenches, seamounts, and accretionary prisms, along with the distribution of volcanoes across Java Island, are shown. Examples of significant earthquakes include the 2021 Malang Mw 6.4 earthquake in the intraslab zone and the 2020 Jepara Mw 6.7 deep-focus earthquake occurring above the mantle.



Zhan, 2020). Geodetic strain rate analysis further confirms high coupling in southern Java (Hanifa et al., **2014**). The Jepara earthquake occurred within the interior of the oceanic slab, driven by processes such as dehydration and serpentinization, which are linked to a decrease in slab density (Widiyantoro et al., 2020; Ribeiro, 2022). Slab dehydration in the Java subduction zone may facilitate seawater infiltration into the oceanic plate, creating conditions favourable for deep-focus earthquakes. From a seismic perspective, nearly all deep-focus earthquakes exhibit a significant compensated linear vector dipole (CLVD) component (Sandanbata et al, 2021). This characteristic is often associated with brittle deformation within the slab, despite the high-pressure and high-temperature environment (Widiyantoro et al., 2020).

The change in fault mechanisms reflects instability in shear forces (Chen and Wen, 2015). This phenomenon is attributed to the polymorphic phase transition of olivine to spinel under deviatoric pressure within the interior of the oceanic plate. This mineralogical transforma-

tion marks the transition from the upper mantle (dominated by olivine) to the mantle transition zone (characterized by spinel), occurring at depths of 410–660 km (Zhan, 2020; Ishii et al., 2021). As a result, fault mechanisms can transform from a thrust faulting mechanism to normal or strike-slip faulting within the mantle transition zone (Chen and Wen, 2015; Zhou et al, 2022). This fault transformation generates structural variations in the mantle transition zone beneath Java Island, leading to distinct seismic source mechanisms at different depths.

4. Conclusions

We successfully highlighted and characterized the July 07, 2020 Jepara earthquake with analyses using moment tensor inversion and hypocenter double-difference relocation. The full-waveform inversion provides an adequate result for all seismic stations used with an error of ~0.5s and a variance reduction of ~60%. The inversion results provide a final magnitude moment at Mw 6.7 at

centroid depth of 544 km and focal mechanism parameter with two nodal planes, the first one with a strike of 310°, a dip of 59°, and a rake of -68°, while the second one has a strike of 92°, a dip of 37°, and a rake of -121°. Furthermore, approximately 85% of the hypocenters were successfully relocated, forming distinct spatial clusters that align with the source mechanism and slab structure of the 2020 Jepara earthquake. Combined analysis of the moment tensor inversion and hypocenter relocation successfully reveals the geometry of the subducting slab and clarifies the position and mechanism of the 2020 Jepara deep-focus earthquake beneath Java Island. The observed normal faulting is likely related to the transition zone, indicating a change in rupture mechanism at depth. These findings enrich tectonic understanding and provide insight for future seismic hazard mitigation in northern Java.

Acknowledgement

We extend our deepest gratitude to the Indonesian Agency for Meteorology, Climatology, and Geophysics (BMKG) for the seismic waveform and hypocentre data and the National Research and Innovation Agency (BRIN) for their outstanding support and contributions to this research. Without the support and facilities provided by BMKG and BRIN, this research would not have been possible. We thank Geophysical Station Office of Karang Panjang, Ambon for letting us to use a well-established program called Automatic Regional Moment Tensor (ARMT). All figures were generated by Generic Mapping Tools (GMT) v.6 (Wessel et al., 2019) and some figures were illustrated with Inkscape v.10.

5. References

- Adi, S.P.; Simanjuntak, A.V.H.; Supendi, P.; et al. (2024). Different faulting of the 2023 (Mw 5.7 and 5.9) South-Central Java earthquakes in the backthrust fault system. Geotechnical and Geological Engineering, 42: 3123–3135. 10.1007/s10706-023-02720-1
- Argus, D.F.; Gordon, R.G. (1991). No-net-rotation model of current plate velocities incorporating plate motion model NUVEL-1. Geophysical Research Letters, 18: 2039–2042. 10.1029/91GL01532
- Asnawi, Y.; Simanjuntak, A.; Muksin, U.; Okubo, M.; Putri, S.I.; Rizal, S.; Syukri, M. (2022). Soil classification in a seismically active environment based on shear wave velocity and HVSR data. Global Journal of Environmental Science and Management, 8(3): 297–314. 10.22034/gjesm.2022.03.01
- Chen, Y.; Wen, L. (2015). Global large deep-focus earth-quakes: Source process and cascading failure of shear instability as a unified physical mechanism. Earth and Planetary Science Letters, 423: 134–144. 10.1016/j.epsl. 2015.04.031
- DeMets, C.; Gordon, R.G.; Argus, D.F. (2010). Geologically current plate motions. Geophysical Journal International, 181: 1–80. 10.1111/j.1365-246X.2009.04491.x

- Gunawan, E.; Widiyantoro, S. (2019). Active tectonic deformation in Java, Indonesia inferred from a GPS-derived strain rate. Journal of Geodynamics, 123: 49–54. 10.1016/j. jog.2019.01.004
- Halauwet, Y.; Afnimar; Triyoso, W.; Vackář, J.; Daryono, D.; Supendi, P.; Hakim, M.L. (2024). A new automated procedure to obtain reliable moment tensor solutions of small to moderate earthquakes (3.0 ≤ M ≤ 5.5) in the Bayesian framework. Geophysical Journal International, 239(2): 1000–1020. 10.1093/gji/ggae309
- Hanifa, N.R.; Sagiya, T.; Kimata, F.; Efendi, J.; Abidin, H.Z.; Meilano, I. (2014). Interplate coupling model off the southwestern coast of Java, Indonesia, based on continuous GPS data in 2008–2010. Earth and Planetary Science Letters, 401: 159–171. 10.1016/j.epsl.2014.06.010
- Ishii, T.; Ohtani, E. (2021). Dry metastable olivine and slab deformation in a wet subducting slab. Nature Geoscience, 14: 526–530. 10.1038/s41561-021-00756-7
- Kennett, B.L.; Engdahl, E.R.; Buland, R. (1995). Constraints on seismic velocities in the Earth from traveltimes. Geophysical Journal International, 122: 108–124. 10.1111/j. 1365-246X.1995.tb03540.x
- Laske, G.; Masters, G.; Ma, Z.; Pasyanos, M. (2013). Update on Crust 1.0: A 1-degree global model of Earth's crust. Geophysical Research. 10.17611/DP/17992676
- Li, J.; Zheng, Y.; Thomsen, L.; Lapen, T.J.; Fang, X. (2018). Deep earthquakes in subducting slabs hosted in highly anisotropic rock fabric. Nature Geoscience, 11: 696–700. 10.1038/s41561-018-0188-3
- Muksin, U.; Arifullah, A.; Simanjuntak, A.V.; Asra, N.; Muzli, M.; Wei, S.; Okubo, M. (2023). Secondary fault system in Northern Sumatra, evidenced by recent seismicity and geomorphic structure. Journal of Asian Earth Sciences, 245: 105557. 10.1016/j.jseaes.2023.105557
- Nugraha, A.D.; Shiddiqi, H.A.; Widiyantoro, S.; Thurber, C.H.; Pesicek, J.D.; Zhang, H.; Wiyono, S.H.; Ramadhan, M.; Wandano; Irsyam, M. (2017). Hypocenter relocation along the Sunda arc in Indonesia, using a 3D seismic velocity model. Seismological Research Letters. 10.1785/ 0220170107
- Pasari, S.; Simanjuntak, A.V.H.; Mehta, A.; et al. (2021a). A synoptic view of the natural time distribution and contemporary earthquake hazards in Sumatra, Indonesia. Natural Hazards, 108: 309–321. 10.1007/s11069-021-04682-0
- Pasari, S.; Simanjuntak, A.V.; Mehta, A.; Sharma, Y. (2021b). The current state of earthquake potential on Java Island, Indonesia. Pure and Applied Geophysics, 178: 2789–2806. 10.1007/s00024-021-02781-4
- Pasari, S.; Simanjuntak, A.V.H.; Neha; et al. (2021c). Now-casting earthquakes in Sulawesi Island, Indonesia. Geoscience Letters, 8: 27. 10.1186/s40562-021-00197-5
- Polet, J.; Kanamori, H. (2000). Shallow subduction zone earthquakes and their tsunamigenic potential. Geophysical Journal International, 142: 684–702. 10.1046/j.1365-246x.2000.00205.x
- Ramírez-Herrera, M.T.; Orozco, J.J.Z. (2002). Coastal uplift and mortality of coralline algae caused by a 6.3 Mw earth-quake, Oaxaca, Mexico. Journal of Coastal Research, 18: 75–81.

- Ribeiro, J.M. (2022). Slab dehydration beneath forearcs: Insights from the southern Mariana and Matthew-Hunter rifts. Geochemical Perspectives Letters, 20: 22–26. 10. 7185/geochemlet.2203
- Sandanbata, O.; Kanamori, H.; Rivera, L.; Zhan, Z.; Watada, S.; Satake, K. (2021). Moment tensors of ring-faulting at active volcanoes: Insights into vertical-CLVD earthquakes at the Sierra Negra Caldera, Galápagos Islands. Journal of Geophysical Research: Solid Earth, 126(6). 10.1029/2021JB021693
- Saputra, H.; Wahyudi, W.; Suardi, I.; Anggraini, A.; Suryanto, W. (2021). The waveform inversion of mainshock and aftershock data of the 2006 M6.3 Yogyakarta earthquake. Geoscience Letters, 8(1): 9. 10.1186/s40562-021-00176-w
- Setiadi, T.A.P.; Daud, Y.; Martha, A.A.; Rohadi, S. (2022). Earthquake relocation using the double difference teleseismic method in the Java region. Jurnal Meteorologi dan Geofisika, 23(1): 23–27. 10.31172/jmg.v23i1.842
- Simanjuntak, A.V.; Palgunadi, K.H.; Supendi, P.; Daryono, D.; Prakoso, T.A.; Muksin, U. (2023). New insight on the active fault system in the Halmahera volcanic arc, Indonesia, derived from the 2022 Tobelo earthquakes. Seismological Research Letters, 94(6): 2586–2594. 10.1785/0220230006
- Simanjuntak, A.V.H.; Ansari, K. (2024). Multivariate hypocenter clustering and source mechanism of 2017 Mw 6.2 and 2019 Mw 6.5 in the South Seram Subduction System. Geotechnical and Geological Engineering, 42: 4303–4316. 10.1007/s10706-024-02780-x
- Simanjuntak, A.V.H.; Palgunadi, K.H.; Supendi, P.; et al. (2024). The western extension of the Balantak Fault revealed by the 2021 earthquake cascade in the central arm of Sulawesi, Indonesia. Geoscience Letters, 11: 35. 10. 1186/s40562-024-00353-7
- Supendi, P.; Winder, T.; Rawlinson, N.; Bacon, C.A.; Palgunadi, K.H.; Simanjuntak, A.; Jatnika, J. (2023). A conjugate fault revealed by the destructive Mw 5.6 (November 21, 2022) Cianjur earthquake, West Java, Indonesia. Journal of Asian Earth Sciences, 257: 105830. 10.1016/j.jseaes.2023.105830
- Tarantola, A. (2005). Inverse problem theory and methods for model parameter estimation. Society for Industrial and Applied Mathematics. 10.1137/1.9780898717921

- Tibi, R.; Wiens, D.A.; Inoue, H. (2003). Remote triggering of deep earthquakes in the 2002 Tonga sequences. Nature, 424: 921–925. 10.1038/nature01903
- Vackář, J.; Burjánek, J.; Gallovič, F.; Zahradník, J.; Clinton, J. (2017). Bayesian ISOLA: New tool for automated centroid moment tensor inversion. Geophysical Journal International, 210: 693–705. 10.1093/gji/ggx158
- Waldhauser, F.; Ellsworth, W.L. (2000). A double-difference earthquake location algorithm: Method and application to the Northern Hayward Fault, California. Bulletin of the Seismological Society of America, 90: 1353–1368. 10. 1785/0120000006
- Waldhauser, F. (2001). HypoDD A program to compute double-difference hypocenter locations. US Geological Survey.
- Walter, T.R.; Wang, R.; Luehr, B.-G.; Wassermann, J.; Behr, Y.; Parolai, S.; Anggraini, A.; Günther, E.; Sobiesiak, M.; Grosser, H.; Wetzel, H.-U.; Milkereit, C.; Sri Brotopuspito, P.J.K.; Harjadi, P.; Zschau, J. (2008). The 26 May 2006 magnitude 6.4 Yogyakarta earthquake south of Mt. Merapi volcano: Did lahar deposits amplify ground shaking and thus lead to the disaster? Geochemistry, Geophysics, Geosystems, 9(5): Q05006. 10.1029/2007GC001810
- Wessel, P.; Luis, J.F.; Uieda, L.A.; Scharroo, R.; Wobbe, F.; Smith, W.H.; Tian, D. (2019). The generic mapping tools version 6. Geochemistry, Geophysics, Geosystems, 20(11): 5556–5564. 10.1029/2019GC008515
- Widiyantoro, S.; Gunawan, E.; Muhari, A.; Rawlinson, N.; Mori, J.; Hanifa, N.R.; et al. (2020). Implications for megathrust earthquakes and tsunamis from seismic gaps south of Java, Indonesia. Scientific Reports, 10: 1–11. 10.1038/ s41598-020-72142-z
- Wu, C.; Takeo, M. (2004). An intermediate deep earthquake rupturing on a dip-bending fault: Waveform analysis of the 2003 Miyagi-ken Oki earthquake. Geophysical Research Letters, 31. 10.1029/2004GL021228
- Zhan, Z. (2020). Mechanisms and implications of deep earth-quakes. Annual Review of Earth and Planetary Sciences, 48: 147–174. 10.1146/annurev-earth-053018-060314
- Zhou, W.-Y.; Hao, M.; Zhang, J.S.; Chen, B.; Wang, R.; Schmandt, B. (2022). Constraining composition and temperature variations in the mantle transition zone. Nature Communications, 13: Article 1094. 10.1038/s41467-022-28795-7

SAŽETAK

Otkrivanje dinamike dubokih potresa: opažanja događaja Mw 6,7 u Jepari 2020. i procesa subdukcije ispod Jave

Potres koji se dogodio u Jepari 2020. godine (Mw 6,7) važan je duboki seizmički događaj zbog subdukcije indijsko-australske ploče ispod otoka Jave. Ova studija istražuje njegove karakteristike korištenjem automatske inverzije momenta tenzora i relokacija metodom dvostrukih razlika na temelju seizmičkih podataka Agencije za meteorologiju, klimatologiju i geofiziku (BMKG). Analizirano je ukupno 1899 potresa zabilježenih između 2010. i 2022. godine, s fokusom na događaje koji su se dogodili na dubini do 600 km. Analiza tenzora momenta otkrila je normalno rasjedanje s dvjema nodalnim ravninama: prva s pružanjem od 310°, nagibom od 59° i kutom otklona od –68°, a druga s pružanjem od 92°, nagibom od 37° i kutom otklona od –121°. Dubina centroida određena je na 544 km, dok je smanjenje varijance (VR) premašilo 60 %, što rezultate klasificira kao visokokvalitetne (kategorija A). Otprilike 85 % hipocentara uspješno je relocirano, te je srednja kvadratna vrijednost (RMS) vremena putovanja vala poboljšana na manje od 1 sekunde. Potres je povezan s dehidratacijom tektonske ploče i polimorfnim faznim prijelazom olivina u spinel pod visokim tlakom i temperaturom. Ti procesi doprinose promjenama u žarišnim mehanizmima potresa i strukturnim varijacijama prijelazne zone plašta. Rezultati poboljšavaju razumijevanje dinamike dubokih potresa ispod Jave i mogu znatno doprinijeti ublažavanju učinaka budućih potresa u Indoneziji.

Ključne riječi:

otok Java, duboki potresi, inverzija momenta tenzora, relokacija metodom dvostruke razlike, dehidratacija tektonske ploče

Author's contribution

Tio Azhar Prakoso Setiadi (Lead researcher, MSc, Geophysicist) designed the study, lead the research, conducted hypocenter analysis, and prepared the initial manuscript draft. **Anne Maria Magdalena Sirait** (Principal investigator, PhD, Geophysicist) provided methodological guidance, finalized all results, visualization and reviewed the final manuscript. **Yehezkiel Halauwet** (Research associate, MSc, Geophysicist) performed the moment tensor analysis and assisted in refining the discussion. **Andrean V. H. Simanjuntak** (Principal investigator, PhD, Geophysicist) collected the data, performed the preliminary analysis, visualization and ensured the accuracy and scientific rigor of the manuscript. **Adi Susilo** (Principal investigator, Prof, Geophysicist) supervised and funded the research, reviewed the final manuscript, and ensured the accuracy and scientific rigor of the manuscript.

All authors have read and agreed to the published version of the manuscript.